Environmental Pollution 316 (2023) 120443

Contents lists available at ScienceDirect

Environmental Pollution

journal homepage: www.elsevier.com/locate/envpol

Spatio-temporal development of the urban heat island in a socioeconomically diverse tropical city

Emma E. Ramsay [a,*], Grant A. Duffy [a,b], Kerrie Burge [c], Ruzka R. Taruc [d], Genie M. Fleming [a], Peter A. Faber [a], Steven L. Chown [a]

[a] School of Biological Sciences, Monash University, Victoria, 3800, Australia
[b] Department of Marine Science, University of Otago, Dunedin, New Zealand
[c] Monash Sustainable Development Institute, Monash University, Victoria, 3800, Australia
[d] RISE Program, Faculty of Public Health, Makassar, Hasanuddin University, Makassar, Indonesia

ARTICLE INFO

This paper has been recommended for acceptance by Prof. Pavlos Kassomenos

Keywords:
Urban heat islands
Informal settlements
Landsat
Remote sensing
Tropics
Urbanisation
Cities
Land cover change

ABSTRACT

Urban heat islands, where temperatures are elevated relative to non-urban surrounds, are near-ubiquitous in cities globally. Yet, the magnitude and form of urban heat islands in the tropics, where heat has a large morbidity and mortality burden, is not well understood, especially for those of urban informal settlements. We used 29 years of Landsat satellite-derived surface temperature, corroborated by *in situ* temperature measurements, to provide a detailed spatial and temporal assessment of urban heat islands in Makassar, Indonesia, a city that is representative of rapidly growing urban settlements across the tropics. Our analysis identified surface urban heat islands of up to 9.2 °C in long-urbanised parts of the city and 6.3 °C in informal settlements, the seasonal patterns of which were driven by change in non-urban areas rather than in urban areas themselves. In recently urbanised areas, the majority of urban heat island increase occurred before land became 50% urbanised, whereas the established heat island in long-urbanised areas remained stable in response to urban expansion. Green and blue space protected some informal settlements from the worst urban heat islands observed across the city and maintenance of such space will be essential to mitigate the growing heat burden from urban expansion and anthropogenic climate change. Settlements further than 4 km from the coast and with Normalised Difference Vegetation Index (NDVI) less than 0.2 had higher surface temperatures, with modelled effects of more than 5 °C. Surface temperature measurements were representative of *in situ* heat exposure, measured in a subset of 12 informal settlements, where mean indoor temperature had the strongest relationship with surface temperature ($R^2 = 0.413$, $P = 0.001$). We advocate for green space to be prioritised in urban planning, redevelopment and informal settlement upgrading programs, with consideration of the unique environmental and socioeconomic context of tropical cities.

1. Introduction

Human populations are rapidly expanding and becoming increasingly urbanised. More than half of the world's population now lives in urban areas and this is expected to increase to nearly 70% by 2050 (United Nations, 2019), accompanied by a near doubling of global urban land cover between 2015 and 2050 (Huang et al. 2019). The majority of this growth will occur in developing countries, particularly in Asia and Africa, home to most of the world's fastest growing cities (Laurance et al. 2015; United Nations, 2019). City growth in these contexts is often characterised by urban informal settlements which typically have poor quality infrastructure and services, and high exposure to environmental hazards (Ezeh et al. 2017). More than one billion people live in informal settlements globally, primarily in East and South-East Asia, a number which is expected to increase with continued population growth and urbanisation (UN-Habitat, 2015; United Nations, 2021a).

The growth of cities drives local change in land cover, climate and hydrological cycles (Grimm et al. 2008). One of the most prominent outcomes of this environmental change is the urban heat island (UHI) effect (Seto & Shepherd, 2009; Bai et al. 2017). Urban heat islands are primarily caused by land cover changes, associated with urbanisation, which alter the surface energy balance and morphology (Oke, 1982;

* Corresponding author.
E-mail address: emma.ramsay1@monash.edu (E.E. Ramsay).

https://doi.org/10.1016/j.envpol.2022.120443
Received 8 August 2022; Received in revised form 5 October 2022; Accepted 12 October 2022
Available online 17 October 2022

Arnfield, 2003). Such land cover change across a broad extent leads to high absorption and retention of radiant heat in urban areas, and thus increased ambient and surface temperature relative to surrounding non-urban areas (Bai et al. 2017). In consequence, these elevated temperatures can exacerbate extreme heat (Founda & Santamouris, 2017; Zhao et al. 2018), which has adverse impacts on human health and wellbeing (Tan et al. 2010; Ebi et al. 2021a). Througout the tropics, UHIs compound year-round high temperature and humidity, which is of particuclar concern for vulnerable populations such as those living in urban informal settlements (Scott et al. 2017; Ramsay et al. 2021) who have limited capacity to adapt (Pasquini et al. 2020) and a large exisiting health burden (Ezeh et al. 2017; Lilford et al. 2017).

Urban heat islands have been relatively well characterised globally (Peng et al. 2012; Chakraborty & Lee, 2019), with advances in remote sensing techniques and data availability accelerating this characterisation (Kotharkar et al. 2018). Yet much of the focus remains on temperate regions of the world including Europe, North America and China (Zhou et al. 2018). Many studies are also limited to simplified comparisons of urban and non-urban areas, or single time-points, which do not sufficiently capture intra-urban variation, temporal trends or local context (Tuholske et al. 2021). Spatial and temporal patterns of urban warming are heterogenous globally, with UHIs influenced by local climatic conditions, city size and density (Imhoff et al. 2010; Li et al. 2017; Miles & Esau, 2020), and variation in urban land use, morphology and socioeconomic factors (Chen et al. 2006; Wang et al. 2019; Tepanosyan et al. 2021). As cities grow, interactions between land use change and socioeconomic development will, therefore, drive changes in UHI magnitude, extent and impacts (Lee et al. 2019; Li et al. 2020). Indeed, evidence is mounting that in some cities, lower income neighbourhoods have disproportionately high exposure to UHIs (Buyantuyev & Wu, 2009; Chakraborty et al. 2019). Such neighbourhoods are likely to include informal settlements, which themselves may be exposed to higher UHIs due to dense housing and limited green space (Mehrotra et al. 2018; Wang et al. 2019), although this may be reduced if settlements are embedded in green or blue space (Jacobs et al. 2019). However, spatially explicit information about informal settlements is scarce (Satterthwaite et al. 2020) and they have been insufficiently considered in UHI analyses.

Ongoing urbanisation and informal settlement growth, coupled with the inherent health and socioeconomic burdens faced by informal settlement residents as the climate warms (Scovronick et al. 2015; Satterthwaite et al. 2020), make mitigating UHIs a growing priority for sustainable development. This priority is reflected in the increasing interest and investment by development banks in nature-based solutions (Hamel and Tan, 2022; RISE & ADB, 2021), which are potentially the most feasible means to limit the extent and impacts of UHIs (Ranagalage et al. 2020; Li et al. 2022) and are a major focus of both the Sustainable Development Goals (United Nations, 2021b) and Planetary Health approaches (Whitmee et al. 2015). The effectiveness of UHI mitigation strategies does, however, depend upon the development of an explicit, localised understanding of the spatial and temporal patterns of UHI exposure in rapidly growing cities and their associated informal settlements (Deilami et al. 2018; Nagendra et al. 2018). Better understanding of trends in urban development and UHIs will facilitate predictions of the potential for spatial expansion and intensification of UHIs (Sejati et al. 2019; Li et al. 2021), allowing new knowledge of spatio-temporal trends to be integrated into context-specific mitigation strategies. Unfortunately, localised understanding of the spatio-temporal patterns of UHI expansion in some of the world's fastest growing cities is lacking, and informal settlements are severely underrepresented in the UHI literature.

Therefore, we have three clear objectives for this study. First, to provide improved understanding of spatio-temporal trends of UHIs. Second, to demonstrate that UHIs not only develop together with urban expansion in tropical cities, but also affect urban informal settlements. Third, to offer empirical insight into what components of city development and nature-based solutions may help to mitigate UHI effects, especially for the urban poor who constitute the majority of informal settlement residents.

We do so by quantifying spatial and temporal patterns of urbanisation and accompanying UHIs over the last 30 years in an exemplar, socioeconomically diverse, tropical South-East Asian city: Makassar, South Sulawesi, Indonesia. Indonesia is one of the most urbanised countries in Asia with 110 million people living in 60 cities (Gunawan et al. 2015) and 30% of the urban population living informally (United Nations, 2021a). Makassar is a medium-sized (<5 million people) city with a population of ~1.5 million people, in this way representing more than 90% of urban settlements globally (United Nations, 2018). Furthermore, Makassar is characterised by a diversity of informal settlements distributed across much of its extent (French et al. 2021) and is the subject of a nature-based informal settlement revitalisation program proposed both for this city and for others (Leder et al. 2021).

2. Materials and methods

Local-scale UHI analyses require data at fine spatial and temporal resolutions. Ambient temperature is preferred for analysing urban heat impacts on humans. Yet climate data from traditional weather stations do not capture localised heat exposure in complex urban settlements (Scott et al. 2017; Ramsay et al. 2021) and are particularly scarce throughout the tropics (Zaitchik & Tuholske, 2021). Satellite data are therefore valuable for fine-scale spatial and temporal analyses where *in situ* data are unavailable (Zhou et al. 2018; Zhu et al. 2019), and have thus been used extensively to characterise UHIs across the globe (e.g., Peng et al. 2012; Estoque et al. 2017; Zhou et al. 2017; Chakraborty & Lee, 2019; Manoli et al. 2019).

We therefore used the 40 year near-global record of multispectral spatial data from the Landsat satellite series, including Landsat 5 TM, Landsat 7 ETM+ and Landsat 8 OLI TIR between 1980 and 2020 (Wulder et al. 2019) to characterise urban land cover and analyse spatial and temporal trends in surface temperature in Makassar, Indonesia (Fig. 1). Landsat data comprise spectral bands in the visible, near infrared, short wave and thermal infrared spectra at a spatial resolution of 30 m (thermal bands are resampled to 30 m), with a 16-day temporal coverage of the earth's surface (Markham & Helder, 2012; Roy et al. 2014). Landsat satellites have an overpass time of approximately 10 a.m. Makassar local time (WITA; UTC+8).

2.1. Urban land cover change

Supervised land cover classifications were performed by E.E.R. for 11 time points between 1993 and 2019 to determine changes in urban land cover over time, and distinguish long-urbanised parts of the city and more recently urbanised areas (Fig. 2). Landsat Collection 1, Level 1 imagery (U.S. Geological Survey, 2019) were downloaded and pre-processed (conversion to reflectance, DOS1 atmospheric correction) using the Semi-Automatic Classification Plugin (version 7.10.5; Congedo, 2016) in QGIS (version 3.4.2; QGIS Development Team, 2018). Images within the dry season months (April to October) were manually selected for land cover classification to minimise seasonal variation in land cover and optimise availability of cloud-free images. Where data from more than one satellite were available, data from the most recently deployed satellite were used, except between 2003 and 2013, where Landsat 5 data were used in place of Landsat 7 data after the failure of the scan line corrector on Landsat 7 (Markham et al. 2004).

The Semi-Automatic Classification Plugin (Congedo, 2016) was used to classify land cover at each time point based on remote-sensed visible spectrum and infrared Landsat bands (Landsat 5 and Landsat 7: Bands 1–5 and 7, Landsat 8: Bands 2–7) using the maximum likelihood classification method. Clouds were masked manually by drawing polygons over areas affected by clouds or their shadows and then images were clipped to a study region which included the urban extent of the city as

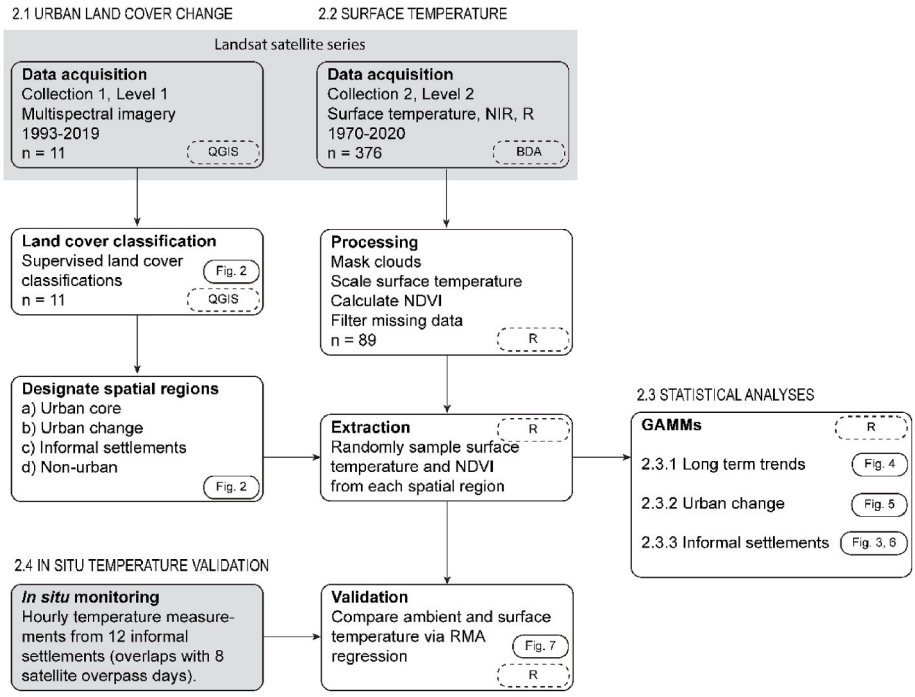

Fig. 1. Summary of methods showing data sources (grey), data processing (software used in dashed boxes) and analyses, indicating the figures corresponding to each stage. Code for analyses are available at https://doi.org/10.26180/21268050.v1. Acronyms: BDA = bulk download application, NIR = near infrared, R = red, NDVI = normalised difference vegetation index, RMA = ranged major axis, GAMM = generalised additive mixed model.

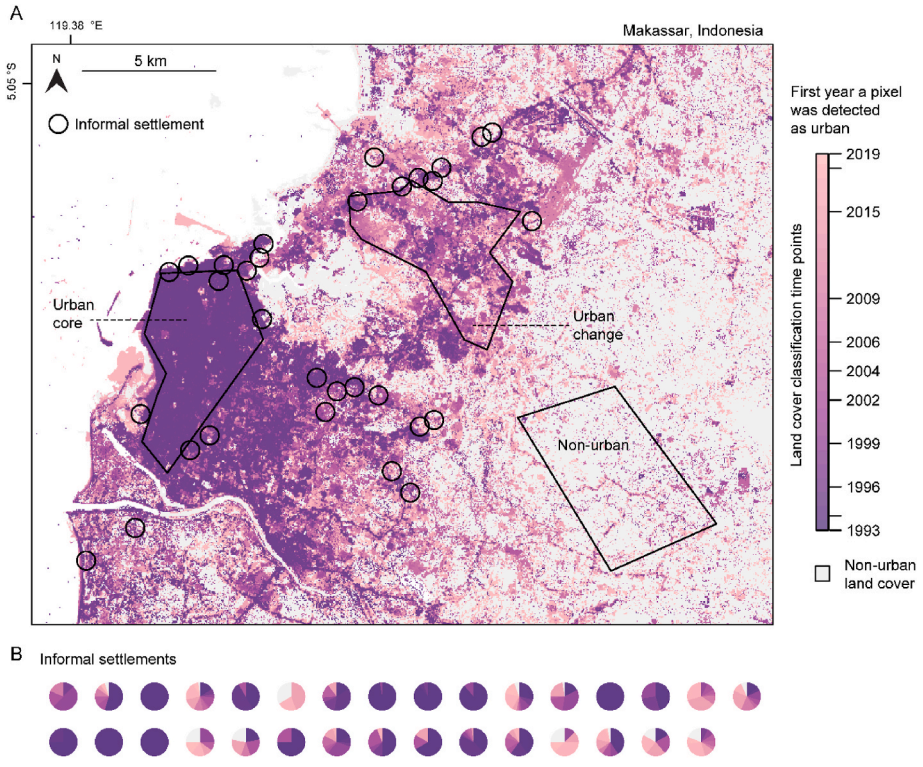

Fig. 2. A) Urban land cover change in Makassar, Indonesia between 1993 and 2019 showing the urban core, urban change, non-urban and informal settlement sampling areas. Informal settlement locations represent the general location of the settlement rather than the exact polygon. Map shows the first year a pixel was detected as urban based on 11 land cover classifications. Legend ticks represent land cover classification time-points. B) The distribution of urban land cover change in 31 informal settlements. Each pie chart represents the first year a pixel was detected as urban in one settlement.

well as a variety of non-urban land cover types for training. The classification algorithm was trained by manually selecting training areas from true and false colour composites of Landsat bands and assigning them to six broad land cover classes: water, urbanised, vegetation, cropland, wet-cropland/wetland and bare soil, based on visual assessment and photointerpretation of the Landsat images. Training areas were a minimum of 60 pixels and a maximum of 1000 pixels, and were selected using the automatic region growing algorithm (Congedo, 2016) to group spectrally similar pixels together. A minimum of 10 training areas were selected for each land cover class and these were spread throughout the image to obtain a representative description of each class (Foody & Mathur, 2004).

Based on changes in urbanised land cover over time (Fig. 2A) we defined four spatial regions for UHI analysis (Fig. 2A):

a) The urban core which was predominantly urbanised at the first land cover classification (June 23, 1993) and remained urbanised over the time period of this study
b) An area of urban change which changed from predominantly non-urban to urbanised over the time period of this study
c) Informal settlements (detailed below)
d) A non-urban area for comparison which comprised primarily non-urban land cover types and remained predominantly non-urban for the entire time period of this study

We manually defined the urban core, urban change and non-urban areas based on the land cover classifications (Fig. 2A), whilst minimising geographical and topographical differences which could confound temperature observations. Informal settlement locations in Makassar were identified from a list of candidate settlements for the Revitalising Informal Settlements and their Environments (RISE) Program (Leder et al. 2021). These settlements were visited and verified as informal settlements by K.B. and represent some of the most vulnerable urban dwellers (French et al. 2021). The initial list included 39 informal settlement locations (including the 12 settlements in the RISE Program and the RISE demonstration site; RISE & ADB, 2021). Where settlements were less than 200 m from each other we grouped them as a single spatial unit, resulting in a final dataset of 31 settlements. The settlements are geographically dispersed across the city, mainly on the periphery of the urban core and in more recently urbanised areas (Fig. 2A). We note that these settlements were selected with the potential to house nature-based infrastructure upgrades on-site (Leder et al. 2021), and thus are mainly low to medium density settlements. The settlements have a mean area of 0.019 km^2, which is comparable to the global average of 0.016 km^2 (Friesen et al. 2018).

2.2. Land surface temperature

From the Landsat satellite archive (Cook et al. 2014), we downloaded all available Landsat Collection 2, Level 2 imagery (aside from Landsat 7 after 2003; U.S. Geological Survey, 2020) for Makassar (path 114, row 64) between 1970 and 2020 using the Earth Explorer Bulk Download Application (https://earthexplorer.usgs.gov/bulk/), totalling 376 time points. Surface temperature and pixel quality rasters were extracted for each time point, scaled and converted from Kelvin to degrees Celsius (U.S. Geological Survey, 2020). Surface temperature rasters were masked using the pixel quality raster by setting pixels identified as clouds or water to NA. We also extracted the red (R) and near-infrared bands (NIR) to calculate the Normalised Difference Vegetation Index (NDVI) as:

$$NDVI = \frac{(NIR - R)}{(NIR + R)} \quad (1)$$

We randomly sampled 31 points within each of the spatial regions (urban core, urban change and non-urban; Fig. 2) and then buffered them (by a radius of 78 m or ~2.6 pixels) to approximately the same size as informal settlements (~21 pixels). This enabled us to achieve a balanced sampling design with the informal settlement locations and minimised the effect of spatial autocorrelation, by analysing a random sample of surface temperature observations rather than all pixels within each region (Buyantuyev & Wu, 2009).

Landsat satellite data are limited by cloud cover, especially during the wet season (November to March) where few cloud free images are available. To maximise data availability for analyses we filtered surface temperature data in two stages. Time points with more than 25% missing data in the general study area (map area in Fig. 2A) and more than 10% of missing data in the sampling areas (Fig. 2A) were excluded. The remaining data were manually checked for cloud contamination not sufficiently masked by the pixel quality raster, by visualising the surface temperature rasters, resulting in 89 time points between 1991 and 2020 available to be included in analyses. Data were filtered for a second time for each set of analyses, based on the data required for each model. We excluded time points where there were more than six missing samples from the 31 patches or informal settlements from any of the spatial regions of interest for the analysis.

Mean surface temperature and NDVI values were extracted for each sampling location (31 informal settlements and 31 randomly sampled patches in each of urban core, urban change and non-urban; Fig. 2) using the *extract* function in the *raster* package (Hijmans, 2020). Land cover from the 11 land cover classifications was also extracted for each and the percentage of urban pixels within the patch computed for each classification. The mean elevation, extracted from the Shuttle Radar Topography Mission (Farr et al. 2007) was between 0 and 30 m for all settlements and random patches.

Unless otherwise stated, all data processing was performed in R (version 4.05; R Core Team, 2021) using the *dplyr* (Wickham et al. 2022), *raster* (Hijmans, 2020), *sf* (Pebesma, 2018) and *rgeos* (Bivand & Rundel, 2020) packages.

2.3. Statistical analyses

Generalised additive mixed models (GAMMs) were used to estimate spatial and temporal trends in surface temperature. Additive models can fit smooth non-linear trends (such as trends over time) and can handle irregular temporal spacing of samples (Simpson, 2018), thus making them suitable for our data. Random effects were incorporated to account for spatial autocorrelation. GAMMs were fit in R using the *mgcv* package (Wood, 2004) with random effects estimated in the *nlme* package (Pinheiro et al. 2021) using restricted maximum likelihood estimation (REML; Wood, 2011). Unless otherwise stated, smooth trends were fit with thin plate regression splines (Wood, 2003). Model selection was based on Akaike's information criterion (AIC).

First, we modelled long-term trends (1991–2020) in surface temperature in the urban core, urban change and non-urban areas to understand if the magnitude of UHIs has changed over time with the growth of the city. Second, we modelled surface temperature in the urban change area separately to understand how change in urban land cover has driven changes in land surface temperature. Third, we quantified and compared current (2017–2020) UHIs in the urban core and informal settlements. Finally, we modelled spatial predictors of surface temperature in informal settlements. We visualised temporal trends and quantified UHIs from fitted data with simultaneous confidence intervals computed by simulating from the posterior distribution of the model using the *gratia* package (Simpson, 2018; Simpson, 2022).

2.3.1. Long-term trends

We modelled surface temperature in the urban core and non-urban areas as smooth functions of the long-term trend as days since first sampling date (with the first sampling date being day one) and the seasonal (within year) pattern modelled as a cubic spline smooth of day of year. Each smooth trend was fitted separately for urban and non-urban data, which lowered AIC compared to models with one trend. Spatial plots of the normalised residuals indicated residual spatial autocorrelation in the model so we added a residual correlation structure, nested within each time point, which improved both visual inspection of plots and AIC. The optimal spatial correlation structure available in *nlme* was selected via AIC.

We fitted the same model as above for surface temperature in the urban change and non-urban areas, with the addition of a smooth (tensor product) interaction between days since first sampling date and day of year to allow for the seasonal trend changing over time with land cover change.

2.3.2. Urban change

Urbanisation occurred at different times across the urban change area (Fig. 2). We therefore wanted to model the temperature trend separately for each randomly sampled patch to understand how UHIs develop as land converts to urban. We fit models following Pedersen et al. (2019) which allowed long-term smooths to be estimated for each urban change patch. The best model included a global smooth for the overall long-term trend and patch-level smooths modelled as a *t2* factor interactions which allowed the shape of the smooth to vary for each patch (Wood et al. 2012). The model included a seasonal smooth and a residual spatial correlation structure as detailed above.

We identified significant periods of change in surface temperature by computing the first derivative of the estimated long-term trends for each patch using the method of finite differences, where the difference between two very close together values is an approximation of the first derivative (Simpson, 2018). We calculated the yearly mean derivative and compared these to the percentage of urban land cover in that year (interpolated linearly between land cover classification dates). Statistically significant periods of change were inferred where simultaneous confidence intervals of the derivative did not include zero (Simpson, 2018).

Data exploration revealed very different shaped trends which seemed to depend on different urban land use in the area of urban change, which is dominated by more industrial areas compared to the urban core (Surya et al. 2021). To differentiate between different land use types we calculated the mean area of building footprints (extracted from Open Street Map; OpenStreetMap contributors, 2022) intersecting each urban change patch. We classified patches as industrial land use where the mean building footprint size was greater than 250 m^2 or as other urban land use when less than 250 m^2. We then manually checked each patch using Google Earth Imagery and reclassified one patch as industrial where large buildings visible on Google Earth Imagery were missing from Open Street Map (see Figure S1 for examples of each land use type).

2.3.3. Informal settlements

To quantify UHIs in the urban core and informal settlements we modelled recent (2017–2020) surface temperature in the urban core, informal settlements and non-urban areas. As in previous models, the seasonal trend was modelled as a smooth cubic spline of day of year, separately for each group, and a residual spatial correlation structure was included, nested within each time point. Seasonal patterns in UHIs (ΔT) were quantified by computing differences between fitted trends (Simpson, 2022). Significant differences in temperature and thus UHIs were inferred where the simultaneous confidence interval of the difference did not include zero (Rose et al. 2012).

To examine spatial variation in UHI magnitude among informal settlements we modelled surface temperature as a smooth function of the mean NDVI of the settlement, the mean NDVI within a 250 m radius surrounding the settlement, and the distance to the coast. As in previous models, the seasonal trend was modelled as a smooth cubic spline of day of year and a residual spatial correlation structure was included, nested within each time point. We fitted the same model with spatial predictors as linear parametric terms and only day of year as a smooth function.

2.4. In situ temperature validation

To understand the extent to which surface temperature is representative of conditions experienced by people living in informal settlements we compared satellite derived surface temperature to *in situ* temperature measurements in a subset of 12 informal settlements. Monitoring was undertaken as a part of the RISE Program (Leder et al. 2021) and is detailed in Ramsay et al. (2021). Hourly temperature was measured by a network of 780 iButton data loggers (Maxim Integrated, San Jose, California), with approximately 60 loggers in houses (six in each of ten houses) and five outdoors in each settlement. Data retrieval was limited by logger loss, logger failure and fieldwork limitations caused by the Covid-19 pandemic. To capture representative conditions in each settlement we only included time periods where data were retrieved from at least two outdoor loggers at a settlement or loggers in at least two houses in a settlement (Table S1).

In situ temperature data that met the above requirements overlapped with eight satellite overpass days (Table S1). For each settlement we calculated daily mean, minimum and maximum ambient temperature, separately for indoors and outdoors, and compared these to the mean surface temperature of the settlement on the same day. Minimum and maximum temperatures were derived by calculating the minimum (maximum) daily temperature for each logger and then taking the mean of the minimum (maximum) values across each settlement.

We compared mean settlement surface temperature with *in situ* derived variables via ranged major axis regression using the R package *lmodel2* (Legendre, 2018). Ranged major axis regression (or model II regression) aims to describe the relationship between x and y where both variables are not controlled by the researcher, and have natural variation and measurement error (Warton et al. 2006; Sokal & Rohlf, 2012). We assumed that the error variance was larger for surface temperature, but proportional to the variance, thus making ranged major axis regression a suitable method for our data. The significance of the ranged major axis slope was tested via permutation (n permutations = 999).

3. Results

3.1. Urban land cover change

In Makassar, urban land cover increased by 175% (annual growth rate of 6.7%), from 65 km^2 in 1993 to 179 km^2 in 2019, across the map area in Fig. 2A. Urban growth occurred primarily to the North-East of the city, where we examined associated change in UHIs. In informal settlements, urban land cover was mixed between recent and long urbanised land (Fig. 2B). Overall, informal settlements comprised between 42.8% and 100% urbanised land cover based on the most recent land classifications (2018 and 2019).

3.2. Urban heat islands

3.2.1. Urban core

The urban core, which represents long-urbanised parts of the city (Fig. 2A), experienced significant UHIs across a typical year (modelled with data between 2017 and 2020), with a strong seasonal dependence (Fig. 3; Table S2). The UHI averaged 4.5 °C across the year, reaching as high as 9.2 °C in February, but becoming a "cool island" by as much as −6.8 °C in October (Fig. 3). Importantly, this seasonal pattern was due to elevated temperature in the non-urban area rather than a decrease in temperature in the urban core (Fig. 3A). Such seasonal trends are consistent across our analyses where surface temperature in urban areas varies little seasonally, but seasonal changes in UHIs are driven by variation in non-urban areas. UHIs in the urban core have remained relatively stable over the last 30 years, with long-term trends in surface temperature showing little change (Fig. 4A).

3.2.2. Urban change

Modelled long-term trends in surface temperature in the area of urban change reveal how UHIs have grown with urban expansion (Fig. 4B). Trends differ by month as the GAMM allowed the seasonal pattern to vary with the long-term trend as land cover changed (Fig. 4B; Table S2). Overall, surface temperature increased over the last 30 years, particularly between January and June where UHIs are largest in the urban core (Fig. 4). In February, for example, the UHI increased from 1.7 °C in 1991 to 10.2 °C in 2020 (Fig. 4B).

Long-term trends modelled for each randomly sampled patch (Table S2) were much more mixed, accounting for the wide confidence intervals in Fig. 4B. The area of urban change is dominated by industrial

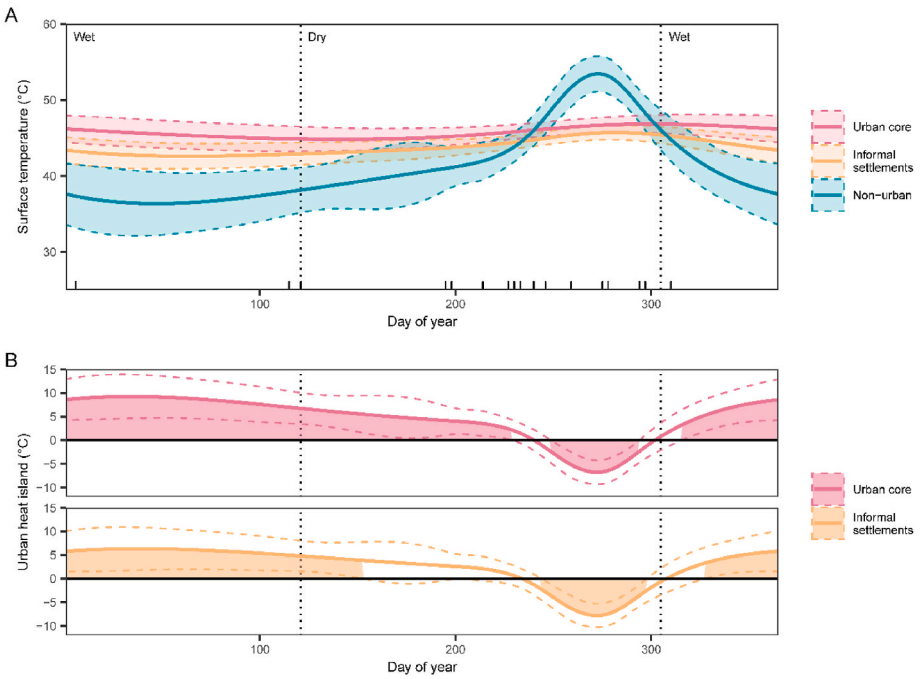

Fig. 3. A) Fitted seasonal trends in surface temperature (2017–2020) with 95% confidence intervals. Ticks above x-axis represent sampling time points. B) Urban heat islands (ΔT) in the urban core and informal settlements. Shading above or below the fitted line indicates significant differences in surface temperature.

land use which is not typical of the urban core (Surya et al. 2021). Trends in industrial areas (mean building footprint >250 m^2), were mixed with periods of both significant increase and decrease, identified from the derivative of the trend (Fig. 5). Trends in other urban areas (mean building footprint <250 m^2), which encompass suburban areas, were much more consistent, showing steady increase in surface temperature, including a period of significant increase (Fig. 5). Across other urban patches, 73% of years where surface temperature increased (positive derivative) occurred before a patch was 50% urbanised, indicating that UHIs establish early on as urban land is converted (Fig. 5B).

3.2.3. *Informal settlements*

UHIs in informal settlements followed a similar seasonal pattern to the urban core but were on average 1.9 °C lower (Fig. 3). UHIs still exceeded 4 °C (averaging 2.6 °C) for much of the year and reached as high as 6.3 °C in February and as low as −7.8 °C in October. The average NDVI within settlements, and surrounding settlements, as well as distance to the coast were important predictors of surface temperature among informal settlements (Fig. 6; Table S2), explaining nearly 40% of the deviance (adj-R^2 = 0.385). Settlements further from the coast had higher surface temperatures, with larger warming effects when further than 4 km and larger cooling effects when within 1 km of the coast (Fig. 6). The NDVI of a settlement had the largest effect, where settlements with NDVI less than 0.2 were considerably warmer (effect of more than 5 °C) than those with NDVI greater than 0.2. For comparison, the mean NDVI of randomly sampled patches in the urban core was 0.22 between 2017 and 2020 (ranging between 0.20 in October and 0.26 in January). The NDVI of the 250 m surrounding each settlement had a smaller effect but settlements surrounded by land with higher NDVI, indicating more green space, were cooler. The inclusion of NDVI as a predictor negated the minimal seasonal effect in informal settlements (Fig. 3A; Fig. 6), indicating that seasonal changes in vegetation are responsible for much of the seasonal variation in surface temperature. The direction of effects was consistent when predictors were modelled as linear parametric terms (Table S3; adj-R^2 = 0.411).

Satellite-derived surface temperature was most strongly related to mean indoor temperature (R^2 = 0.413, P = 0.001) in informal settlements, though relationships with indoor minimum, indoor maximum, outdoor maximum and outdoor mean temperature were also positive and significant (Fig. 7). In all cases, the slope of the line was greater than one, where small increases in ambient temperature are associated with larger change in surface temperature. Although the relationship is not one to one, this does suggest that satellite-derived UHIs can predict heat stress experienced by residents of informal settlements, under cloud-free conditions, where elevated surface temperature is representative of hot ambient conditions.

4. Discussion

Over the past 30 years urban land cover in Makassar has nearly tripled, accompanied by the spatial expansion of UHIs, which affect large parts of the city, including informal settlements. Annual increase in urban land cover of 6.7% exceeded global rates of 3.5% over the same time period, although was less than estimates of 10.8% for Indonesia as a whole, which included larger cities (He et al. 2018). Urban heat islands in Makassar averaged 4.5 °C annually in the urban core, and 2.6 °C in informal settlements, although with seasonal fluctuations they reached maxima of 9.2 °C and 6.3 °C above non-urban surface temperature, respectively. These well exceed annual average satellite-derived surface UHIs of 1.3 °C in the tropics (Chakraborty & Lee, 2019) or 1.2 °C in Asia (Peng et al. 2012), reported by global studies which make simplified comparisons between urban and non-urban pixels within an urban extent. Our results are more in line with surface UHIs between 5 °C and 8 °C detected in South-East Asian megacities, Bangkok, Manila & Ho Chi Minh, during the dry season (Tran et al. 2006). They highlight that smaller cities, and informal settlements within these, are not exempt from UHIs, and the likely impacts thereof, that have been observed in larger cities. Exposure to elevated temperature has direct effects on health and wellbeing (Mendez-Lazaro et al. 2018; Ebi et al. 2021b), exacerbates socioeconomic stressors (Tran et al. 2013), especially for informal settlement residents, and is expected to continue doing so. The anthropogenic heat burden has already been responsible, on average, for 37% of warm-season heat-related deaths globally (Vicedo-Cabrera et al. 2021).

In contrast to previous studies (Chakraborty et al. 2019; Jacobs et al. 2019), which identified elevated UHIs in lower income neighbourhoods

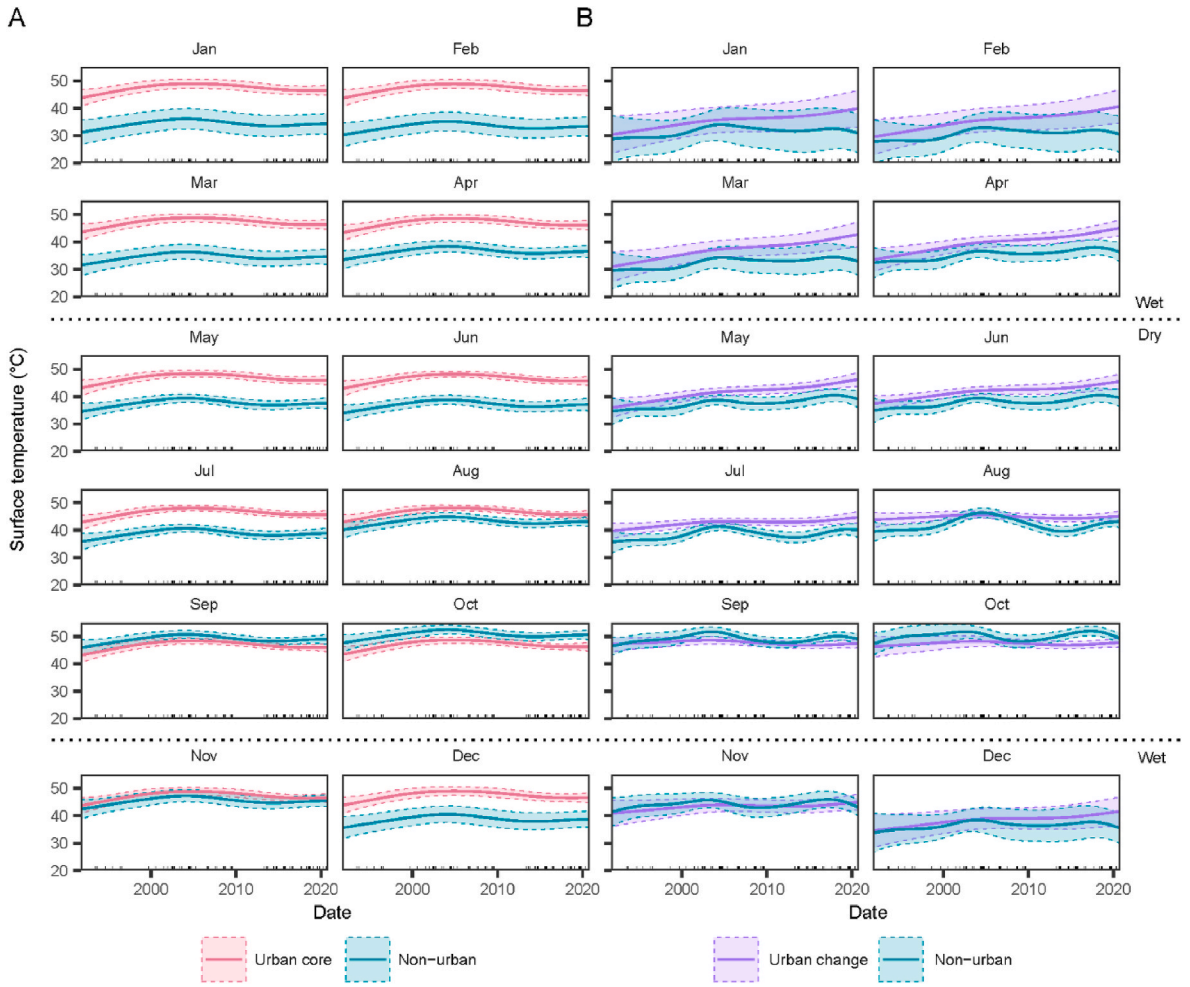

Fig. 4. Fitted long-term trends in surface temperature for each month with 95% confidence intervals in A) the urban core and non-urban areas and B) urban change and non-urban areas. Fitted trends were computed for the 15th day of each month. Ticks above the x-axes represent sampling time points included in the model.

within cities, we found that UHIs in informal settlements were on average 1.93 °C lower across a year than the urban core (representative of formal settlements), although other informal settlements, not included in this study, may experience a higher heat burden if located in densely urbanised parts of the urban core. Despite the smaller magnitude of UHIs overall, residents of informal settlements are especially vulnerable to heat due to poor quality housing, a large existing health burden and occupational heat exposure (Tran et al. 2013; Ezeh et al. 2017). Green space in, and surrounding settlements, along with proximity to the coast appeared to protect some informal settlements from the worst UHIs. Green space has a cooling effect both through shading and evapotranspiration (Aflaki et al. 2017), although the cooling potential from evapotranspiration is upper bounded by high humidity in the tropics (Yu et al. 2018; Manoli et al. 2019; Cuthbert et al. 2022). Meanwhile, large water bodies, including oceans and lakes, have a cooling effect due to the temperature differential between land and water producing cool onshore breezes during the day (Bonan, 2002; Adams & Smith, 2014; Cai et al. 2018). Settlements with NDVI close to that of the urban core (~0.2) were around 5 °C warmer than settlements with more green space. Settlements within 2 km of the coast also had lower temperatures, with cooling effects of up to 5 °C (Fig. 6), although these settlements may be at higher risk of other environmental hazards such as flooding or sea-level rise (Satterthwaite et al. 2020). Based on the relationship with mean indoor temperature, surface temperature differences of 5 °C, from proximity to green or blue space, could represent indoor cooling or heating of more than 1 °C.

It is typically thought that UHIs increase in magnitude as a city increases in size and population (Li et al. 2017; Zhou et al. 2017; Mentaschi et al. 2022), though this effect is smaller in tropical cities (Manoli et al. 2019). We found that UHIs in long-urbanised areas in Makassar have remained stable since at least the 1990s, in line well-researched cities such as London (Jones & Lister, 2009), but have expanded into recently urbanised areas, following patterns observed across Europe (Trusilova et al. 2009) and Africa (Li et al. 2021). Patterns of UHI development in recently urbanised areas varied with urban land use. Industrial areas unexpectedly declined in surface temperature as patches became urbanised, likely due to the form of industrial buildings which have light coloured, high albedo roofs that reflect heat, and the large size of which can create shade and reduce impervious ground surfaces (Connors et al. 2012). By contrast, in other urban patches, which include suburban areas, UHIs develop early on as land becomes urban, with nearly three quarters of surface temperature increase occurring before a patch became 50% urbanised, after which trends stabilised. Given that 70% of new urban land through to 2050 is projected to occur in the tropics (Huang et al. 2019), a large portion of which is likely to include informal settlements (Satterthwaite et al. 2020), the spatial extent of UHIs is likely to increase substantially. It may, therefore, be preferable to prioritise development, including heat mitigation strategies, of partially urbanised land where UHIs have already developed. Reducing urban sprawl not only limits the spatial expansion of UHIs but also has positive effects for biodiversity by reducing habitat loss (Simkin et al. 2022).

Across our results, seasonal patterns of UHIs were driven by increased temperature in September and October in non-urban areas,

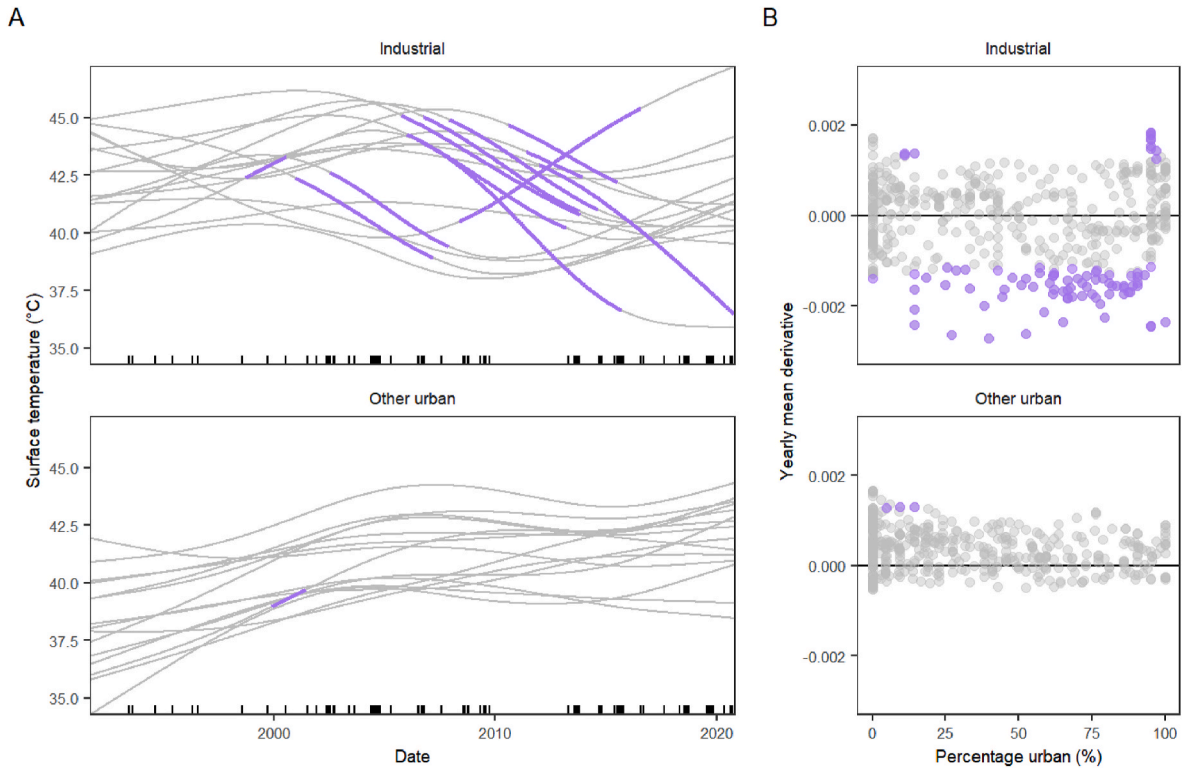

Fig. 5. A) Fitted long-term trends in surface temperature in randomly sampled urban change patches, split by industrial and other urban areas. Fitted trends were computed on the 183rd day of the year. Ticks above the x-axes represent sampling time points included in the model. B) Yearly mean derivative of the long-term trend and the percentage urban land cover of the patch in that year. Significant periods of change, identified from the derivative of the trend, are highlighted in purple.

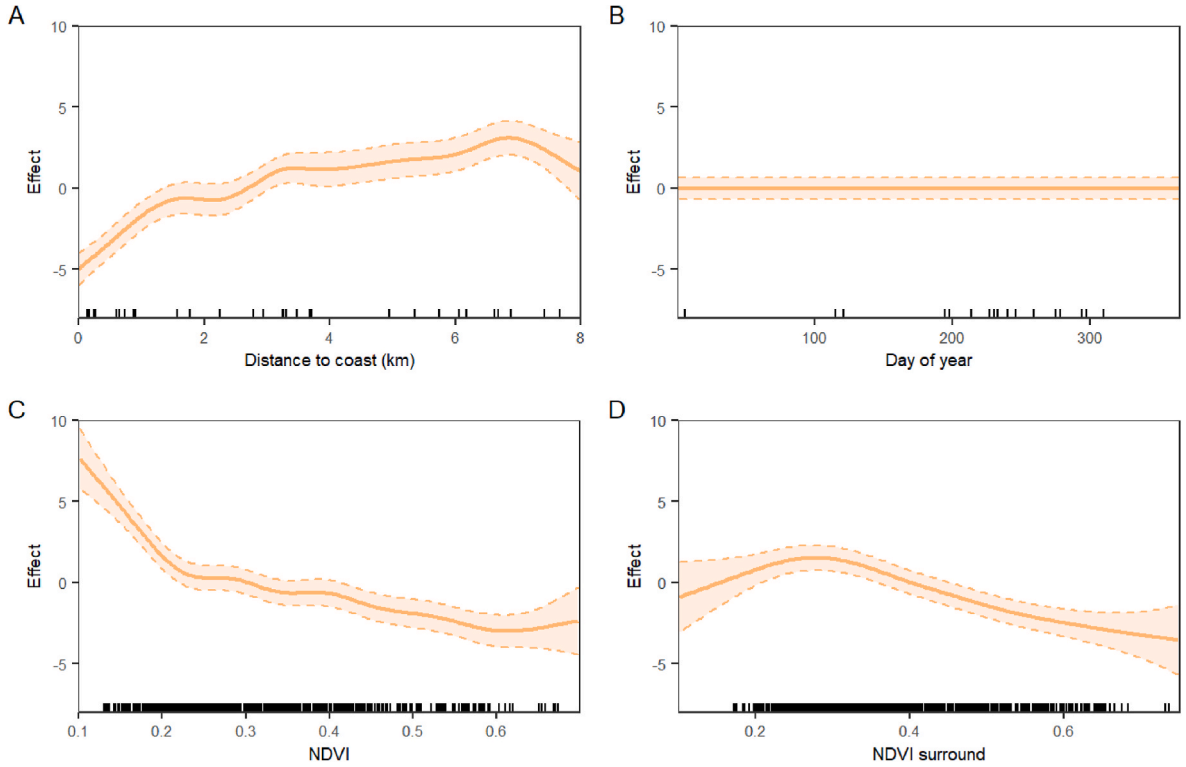

Fig. 6. Modelled effects of predictors of surface temperature in informal settlements for A) distance to coast, B) seasonal trend, C) mean NDVI of a settlement and D) mean NDVI within 250 m radius surrounding the settlement. Ticks above the x-axes represent sampling points included in the model.

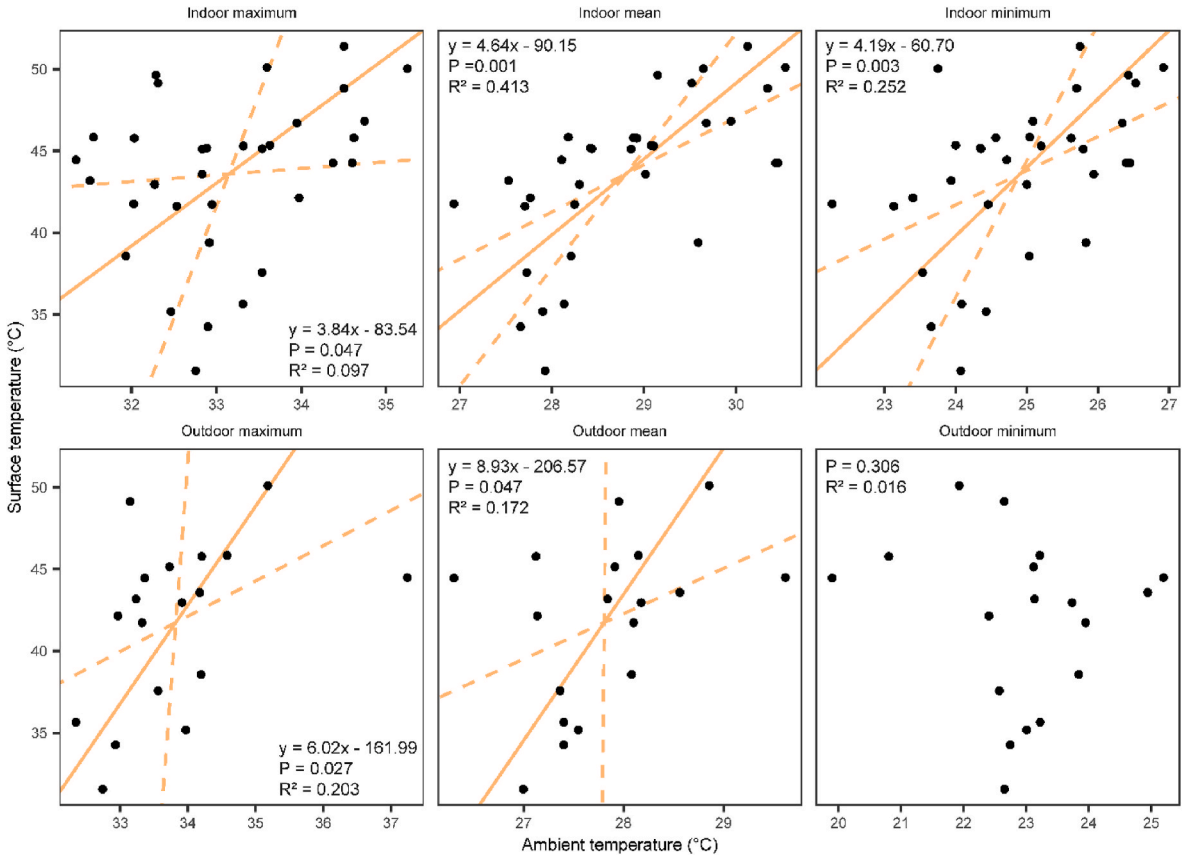

Fig. 7. Ranged major axis regression and 95% confidence intervals (dashed) of daily *in situ* ambient temperature variables and satellite-derived surface temperature in a subset of 12 informal settlements with the regression equation, p-values and R^2. The regression equation is not shown where $P > 0.05$ and R^2 close to zero.

whilst surface temperature in urban areas was relatively stable year-round (Fig. 3; Fig. 4). This is in line with previous work suggesting that the magnitude of UHIs is largely controlled by greening in non-urban areas, which increases the temperature differential with urban areas (Yao et al. 2019). For example, we observed the largest UHIs in the wet season when non-urban, primarily agricultural, areas are most green (See Figure S2 for monthly plots of non-urban NDVI in Makassar). Towards the end of the dry season, in September and October, however, NDVI declines substantially (Figure S2) as crops are harvested and soil moisture declines (Pandey et al. 2014; Kumar et al. 2017). Whilst this technically creates an urban 'cool island', relative to the extremely high surface temperatures recorded from predominantly bare earth in the non-urban area (mean 50.7 °C in September and October, from modelled data), surface temperatures in urban areas remained stable and high (mean 46.6 °C in September and October).

Our results highlight the importance of intra-urban analyses to understand spatio-temporal patterns of UHIs and accurately quantify exposure. Mixed long-term trends with urban land use would otherwise be obscured by coarser resolution data or simplified urban – non-urban comparisons. Fine scale data is also essential for understanding UHIs in informal settlements. Even the Moderate Resolution Imaging Spectroradiometer (MODIS), one of the most common sources of remote sensed surface temperature data (Kotharkar et al. 2018), with a spatial resolution of 1 km^2 is too coarse to detect patterns across informal settlements which have an average size of 0.016 km^2 (Friesen et al. 2018). Whilst satellite derived surface temperature is not a perfect representation of heat stress experienced by people (Venter et al. 2021), we show that it has a reasonable, although not one to one relationship, with *in situ* temperature measured in 12 informal settlements. Impetus is growing for local meteorological monitoring to capture microclimate across complex landscapes, including cities (Zaitchik & Tuholske, 2021). Such data can be collected through low-cost sensor networks (as used here) which have been successful in the informal settlement context (Scott et al. 2017; Ramsay et al. 2021; Van de Walle et al. 2022) and can be used to corroborate and supplement remote-sensed data (Venter et al. 2020). Indeed, such information is essential to understand the magnitude and mechanisms of UHIs in informal settlements globally, and the interactions they may have with climate warming and changing temperature extremes (Chapman et al. 2017).

5. Conclusions

If the ambitions of the Sustainable Development Goals and Planetary Health movements are to be met, heat mitigation must be prioritised and targeted where large UHIs intersect with vulnerable communities. Our results demonstrate large UHIs across a socioeconomically diverse tropical city, which emerge rapidly as land is urbanised. Given that UHIs tend to stabilise after land becomes 50% urbanised, the development of partially urbanised areas should be prioritised to spatially constrain UHIs, with consideration of maintaining green space, which mitigates the worst UHIs. Informal settlements, which are often the subject of redevelopment and upgrading programs, represent an opportunity to explicitly consider green space and other heat mitigation strategies such as ventilation and reflective surfaces (Nutkiewicz et al. 2018; Kimemia et al. 2020). Upgrades, whether nature-based or otherwise, should balance the socioeconomic benefits of built infrastructure, such as roads, with the need to maintain green space. Nature-based solutions offer a compromise where infrastructure upgrades, such as constructed wetlands to improve water and sanitation, can provide co-benefits of heat mitigation by maintaining green and blue space (Wong et al. 2020; Leder et al. 2021; Hamel & Tan, 2022). Such localised interventions will be essential for not only improved local conditions but ongoing climate

resilience (Estrada et al. 2017), especially given the already high anthropogenic heat mortality burden (Vicedo-Cabrera et al. 2021) and forecasts for average global temperature increases of at least 2 °C over the coming decades (Meinshausen et al. 2022).

Ethical statement

Ethics review and approval was provided by participating universities and local IRBs, including Monash University Human Research Ethics Committee (Melbourne, Australia; protocol 9396) and the Ministry of Research, Technology and Higher Education Ethics Committee of Medical Research at the Faculty of Medicine, Universitas Hasanuddin (Makassar, Indonesia; protocol UH18020110). The RISE program is a randomised control trial registered on the Australian New Zealand Clinical Trials Registry (ANZCTR) (Trial ID: ACTRN12618000633280).

Credit authors statement

Emma E. Ramsay: Conceptualisation; Investigation; Data curation; Methodology; Software; Writing – original draft. **Grant A. Duffy**: Conceptualisation; Investigation; Data curation; Methodology; Writing – original draft. **Kerrie Burge**: Investigation; Writing – review & editing. **Ruzka R. Taruc**: Investigation; Project administration; Writing – review & editing. **Genie M. Fleming**: Investigation; Data curation; Writing – review & editing. **Peter A. Faber**: Investigation; Writing – review & editing. **Steven L. Chown**: Conceptualisation; Supervision; Methodology; Writing – original draft.

Declaration of competing interest

The authors declare that they have no known competing financial interests or personal relationships that could have appeared to influence the work reported in this paper.

Data availability

Data and code are deposited in the Monash Figshare Repository https://doi.org/10.26180/21268050.v1. Landsat satellite data are freely available from the United States Geological Survey.

Acknowledgements

The RISE program is funded by the Wellcome Trust [OPOH grant 205222/Z/16/Z], the New Zealand Ministry of Foreign Affairs and Trade, the Australian Department of Foreign Affairs and Trade, the Asian Development Bank, the Government of Fiji, the City of Makassar and Monash University, and involves partnerships and in-kind contributions from the Cooperative Research Centre for Water Sensitive Cities, Fiji National University, Hasanuddin University, Southeast Water, Melbourne Water, Live and Learn Environmental Education, UN-Habitat, UNU-IIGH, WaterAid International and Oxfam. E.E.R is supported by an Australian Government Research Training Program Scholarship. G.A.D. is the recipient of an Australian Research Council Discovery Early Career Researcher Award (DE190100003) funded by the Australian Government. We thank the RISE Program Consortium (details of the RISE study can be found on the study website: www.rise-program.org/) for field data collection assistance and administrative support. Two anonymous reviewers are thanked for their insightful comments.

Appendix A. Supplementary data

Supplementary data to this article can be found online at https://doi.org/10.1016/j.envpol.2022.120443.

References

Adams, M.P., Smith, P.L., 2014. A systematic approach to model the influence of the type and density of vegetation cover on urban heat using remote sensing. Landsc. Urban Plann. 132, 47–54.
Aflaki, A., Mirnezhad, M., Ghaffarianhoseini, A., Ghaffarianhoseini, A., Omrany, H., Wang, Z.-H., Akbari, H., 2017. Urban heat island mitigation strategies: a state-of-the-art review on Kuala Lumpur, Singapore and Hong Kong. Cities 62, 131–145.
Arnfield, A.J., 2003. Two decades of urban climate research: a review of turbulence, exchanges of energy and water, and the urban heat island. Int. J. Climatol. 23, 1–26.
Bai, X., McPhearson, T., Cleugh, H., Nagendra, H., Tong, X., Zhu, T., Zhu, Y.-G., 2017. Linking urbanization and the environment: conceptual and empirical advances. Annu. Rev. Environ. Resour. 42, 215–240.
Bivand, R., Rundel, C., 2020. rgeos: interface to geometry engine- open source ('GEOS'). R Package Version 0.5-5. In: https://CRAN.R-project.org/package=rgeos.
Bonan, G., 2002. Ecological Climatology. University Press, Cambridge United Kingdom.
Buyantuyev, A., Wu, J., 2009. Urban heat islands and landscape heterogeneity: linking spatiotemporal variations in surface temperatures to land-cover and socioeconomic patterns. Landsc. Ecol. 25, 17–33.
Cai, Z., Han, G., Chen, M., 2018. Do water bodies play an important role in the relationship between urban form and land surface temperature? Sustain. Cities Soc. 39, 487–498.
Chakraborty, T., Hsu, A., Manya, D., Sheriff, G., 2019. Disproportionately higher exposure to urban heat in lower-income neighborhoods: a multi-city perspective. Environ. Res. Lett. 14, 105003.
Chakraborty, T., Lee, X., 2019. A simplified urban-extent algorithm to characterize surface urban heat islands on a global scale and examine vegetation control on their spatiotemporal variability. Int. J. Appl. Earth Obs. Geoinf. 74, 269–280.
Chapman, S., Watson, J.E.M., Salazar, A., Thatcher, M., McAlpine, C.A., 2017. The impact of urbanization and climate change on urban temperatures: a systematic review. Landsc. Ecol. 32, 1921–1935.
Chen, X.-L., Zhao, H.-M., Li, P.-X., Yin, Z.-Y., 2006. Remote sensing image-based analysis of the relationship between urban heat island and land use/cover changes. Rem. Sens. Environ. 104, 133–146.
Congedo, L., 2016. Semi-automatic classification plugin documentation. Release 5.3.6.1. https://doi.org/10.13140/RG.2.2.29474.02242/1.
Connors, J.P., Galletti, C.S., Chow, W.T.L., 2012. Landscape configuration and urban heat island effects: assessing the relationship between landscape characteristics and land surface temperature in Phoenix, Arizona. Landsc. Ecol. 28, 271–283.
Cook, M., Schott, J., Mandel, J., Raqueno, N., 2014. Development of an operational calibration methodology for the Landsat thermal data archive and initial testing of the atmospheric compensation component of a land surface temperature (LST) product from the archive. Rem. Sens. 6, 11244–11266.
Cuthbert, M.O., Rau, G.C., Ekstrom, M., O'Carroll, D.M., Bates, A.J., 2022. Global climate-driven trade-offs between the water retention and cooling benefits of urban greening. Nat. Commun. 13, 518.
Deilami, K., Kamruzzaman, M., Liu, Y., 2018. Urban heat island effect: a systematic review of spatio-temporal factors, data, methods, and mitigation measures. Int. J. Appl. Earth Obs. Geoinf. 67, 30–42.
Ebi, K.L., Capon, A., Berry, P., Broderick, C., de Dear, R., Havenith, G., Honda, Y., Kovats, R.S., Ma, W., Malik, A., et al., 2021a. Hot weather and heat extremes: health risks. Lancet 398, 698–708.
Ebi, K.L., Vanos, J., Baldwin, J.W., Bell, J.E., Hondula, D.M., Errett, N.A., Hayes, K., Reid, C.E., Saha, S., Spector, J., et al., 2021b. Extreme weather and climate change: population health and health system implications. Annu. Rev. Publ. Health 42, 293–315.
Estoque, R.C., Murayama, Y., Myint, S.W., 2017. Effects of landscape composition and pattern on land surface temperature: an urban heat island study in the megacities of Southeast Asia. Sci. Total Environ. 577, 349–359.
Estrada, F., Botzen, W.J.W., Tol, R.S.J., 2017. A global economic assessment of city policies to reduce climate change impacts. Nat. Clim. Change 7, 403–406.
Ezeh, A., Oyebode, O., Satterthwaite, D., Chen, Y.-F., Ndugwa, R., Sartori, J., Mberu, B., Melendez-Torres, G.J., Haregu, T., Watson, S.I., et al., 2017. The history, geography, and sociology of slums and the health problems of people who live in slums. Lancet 389, 547–558.
Farr, T.G., Rosen, P.A., Caro, E., Crippen, R., Duren, R., Hensley, S., Kobrick, M., Paller, M., Rodriguez, E., Roth, L., et al., 2007. The Shuttle Radar Topography Mission. Rev. Geophys. 45, RG2004.
Foody, G.M., Mathur, A., 2004. Toward intelligent training of supervised image classifications: directing training data acquisition for SVM classification. Rem. Sens. Environ. 93, 107–117.
Founda, D., Santamouris, M., 2017. Synergies between urban heat island and heat waves in Athens (Greece), during an extremely hot summer (2012). Sci. Rep. 7, 10973.
French, M.A., Fiona Barker, S., Taruc, R.R., Ansariadi, A., Duffy, G.A., Saifuddaolah, M., Zulkifli Agussalim, A., Awaluddin, F., Zainal, Z., Wardani, J., et al., 2021. A planetary health model for reducing exposure to faecal contamination in urban informal settlements: baseline findings from Makassar, Indonesia. Environ. Int. 155, 106679.
Friesen, J., Taubenböck, H., Wurm, M., Pelz, P.F., 2018. The similar size of slums. Habitat Int. 73, 79–88.
Grimm, N.B., Faeth, S.H., Golubiewski, N.E., Redman, C.L., Wu, J., Bai, X., Briggs, J.M., 2008. Global change and the ecology of cities. Science 319, 756–760.
Gunawan, I., Sagala, S., Amin, S., Zawani, H., Mangunsong, R., 2015. City Risk Diagnostic for Urban Resilience in Indonesia. The World Bank, Jakarta, Indonesia.

Hamel, P., Tan, L., 2022. Blue-green infrastructure for flood and water quality management in Southeast Asia: evidence and knowledge gaps. Environ. Manag. 69, 699–718.
He, C., Liu, Z., Gou, S., Zhang, Q., Zhang, J., Xu, L., 2018. Detecting global urban expansion over the last three decades using a fully convolutional network. Environ. Res. Lett. 14, 034008.
Hijmans, R.J., 2020. raster: geographic analysis and modeling with raster data. R package version 3.4-5. http://CRAN.R-project.org/package=raster.
Huang, K., Li, X., Liu, X., Seto, K.C., 2019. Projecting global urban land expansion and heat island intensification through 2050. Environ. Res. Lett. 14, 114037.
Imhoff, M.L., Zhang, P., Wolfe, R.E., Bounoua, L., 2010. Remote sensing of the urban heat island effect across biomes in the continental USA. Rem. Sens. Environ. 114, 504–513.
Jacobs, C., Singh, T., Gorti, G., Iftikhar, U., Saeed, S., Syed, A., Abbas, F., Ahmad, B., Bhadwal, S., Siderius, C., 2019. Patterns of outdoor exposure to heat in three South Asian cities. Sci. Total Environ. 674, 264–278.
Jones, P.D., Lister, D.H., 2009. The urban heat island in Central London and urban-related warming trends in Central London since 1900. Weather 64, 323–327.
Kimemia, D., Van Niekerk, A., Annegarn, H., Seedat, M., 2020. Passive cooling for thermal comfort in informal housing. J. Energy South Afr. 31, 28–39.
Kotharkar, R., Ramesh, A., Bagade, A., 2018. Urban heat island studies in South Asia: a critical review. Urban Clim. 24, 1011–1026.
Kumar, R., Mishra, V., Buzan, J., Kumar, R., Shindell, D., Huber, M., 2017. Dominant control of agriculture and irrigation on urban heat island in India. Sci. Rep. 7, 14054.
Laurance, W.F., Peletier-Jellema, A., Geenen, B., Koster, H., Verweij, P., Van Dijck, P., Lovejoy, T.E., Schleicher, J., Van Kuijk, M., 2015. Reducing the global environmental impacts of rapid infrastructure expansion. Curr. Biol. 25, 259–262.
Leder, K., Openshaw, J.J., Allotey, P., Ansariadi, A., Barker, S.F., Burge, K., Clasen, T.F., Chown, S.L., Duffy, G.A., Faber, P.A., et al., 2021. Study design, rationale and methods of the Revitalising Informal Settlements and their Environments (RISE) study: a cluster randomised controlled trial to evaluate environmental and human health impacts of a water-sensitive intervention in informal settlements in Indonesia and Fiji. BMJ Open 11, e042850.
Lee, K., Kim, Y., Sung, H.C., Ryu, J., Jeon, S.W., 2019. Trend analysis of urban heat island intensity according to urban area change in Asian mega cities. Sustainability 12, 112.
Legendre, P., 2018. lmodel2: model II regression. R Package Version 1.7-3. In: https://CRAN.R-project.org/package=lmodel2.
Li, X., Stringer, L.C., Chapman, S., Dallimer, M., 2021. How urbanisation alters the intensity of the urban heat island in a tropical African city. PLoS One 16, e0254371.
Li, X., Stringer, L.C., Dallimer, M., 2022. The role of blue green infrastructure in the urban thermal environment across seasons and local climate zones in East Africa. Sustain. Cities Soc. 80, 103798.
Li, X., Zhou, Y., Asrar, G.R., Imhoff, M., Li, X., 2017. The surface urban heat island response to urban expansion: a panel analysis for the conterminous United States. Sci. Total Environ. 605–606, 426–435.
Li, Y., Sun, Y., Li, J., Gao, C., 2020. Socioeconomic drivers of urban heat island effect: empirical evidence from major Chinese cities. Sustain. Cities Soc. 63, 102425.
Lilford, R.J., Oyebode, O., Satterthwaite, D., Melendez-Torres, G.J., Chen, Y.-F., Mberu, B., Watson, S.I., Sartori, J., Ndugwa, R., Caiaffa, W., et al., 2017. Improving the health and welfare of people who live in slums. Lancet 389, 559–570.
Manoli, G., Fatichi, S., Schlapfer, M., Yu, K., Crowther, T.W., Meili, N., Burlando, P., Katul, G.G., Bou-Zeid, E., 2019. Magnitude of urban heat islands largely explained by climate and population. Nature 573, 55–60.
Markham, B.L., Helder, D.L., 2012. Forty-year calibrated record of earth-reflected radiance from Landsat: a review. Rem. Sens. Environ. 122, 30–40.
Markham, B.L., Storey, J.C., Williams, D.L., Irons, J.R., 2004. Landsat sensor performance: history and current status. IEEE Trans. Geosci. Rem. Sens. 42, 2691–2694.
Mehrotra, S., Bardhan, R., Ramamritham, K., 2018. Urban informal housing and surface urban heat island intensity. Environ. Urban. ASIA 9, 158–177.
Meinshausen, M., Lewis, J., McGlade, C., Gutschow, J., Nicholls, Z., Burdon, R., Cozzi, L., Hackmann, B., 2022. Realization of Paris Agreement pledges may limit warming just below 2 degrees C. Nature 604, 304–309.
Mendez-Lazaro, P.A., Perez-Cardona, C.M., Rodriguez, E., Martinez, O., Taboas, M., Bocanegra, A., Mendez-Tejeda, R., 2018. Climate change, heat, and mortality in the tropical urban area of San Juan, Puerto Rico. Int. J. Biometeorol. 62, 699–707.
Mentaschi, L., Duveiller, G., Zulian, G., Corbane, C., Pesaresi, M., Maes, J., Stocchino, A., Feyen, L., 2022. Global long-term mapping of surface temperature shows intensified intra-city urban heat island extremes. Global Environ. Change 72, 102441.
Miles, V., Esau, I., 2020. Surface urban heat islands in 57 cities across different climates in northern Fennoscandia. Urban Clim. 31, 100575.
Nagendra, H., Bai, X., Brondizio, E.S., Lwasa, S., 2018. The urban south and the predicament of global sustainability. Nat. Sustain. 1, 341–349.
Nutkiewicz, A., Jain, R.K., Bardhan, R., 2018. Energy modeling of urban informal settlement redevelopment: exploring design parameters for optimal thermal comfort in Dharavi, Mumbai, India. Appl. Energy 231, 433–445.
Oke, T.R., 1982. The energetic basis of the urban heat island. Q. J. R. Meteorol. Soc. 108, 1–24.
OpenStreetMap contributors, 2022. OpenStreetMap Data Sulawesi, Indonesia. Geofabrik OpenStreetMap data extracts.
Pandey, A.K., Singh, S., Berwal, S., Kumar, D., Pandey, P., Prakash, A., Lodhi, N., Maithani, S., Jain, V.K., Kumar, K., 2014. Spatio-temporal variations of urban heat island over Delhi. Urban Clim. 10, 119–133.
Pasquini, L., van Aardenne, L., Godsmark, C.N., Lee, J., Jack, C., 2020. Emerging climate change-related public health challenges in Africa: a case study of the heat-health vulnerability of informal settlement residents in Dar es Salaam, Tanzania. Sci. Total Environ. 747, 141355.
Pebesma, E., 2018. Simple features for R: standardized support for spatial vector data. R. J. 10, 439–446.
Pedersen, E.J., Miller, D.L., Simpson, G.L., Ross, N., 2019. Hierarchical generalized additive models in ecology: an introduction with mgcv. PeerJ 7, e6876.
Peng, S., Piao, S., Ciais, P., Friedlingstein, P., Ottle, C., Breon, F.M., Nan, H., Zhou, L., Myneni, R.B., 2012. Surface urban heat island across 419 global big cities. Environ. Sci. Technol. 46, 696–703.
Pinheiro, J., Bates, D., DebRoy, S., Sarkar, D., R Core Team, 2021. nlme: linear and nonlinear mixed effects models. R package version 3, 1–152.
QGIS Development Team, 2018. In: QGIS Geographic Information System. Open Source Geospatial Foundation Project.
R Core Team, 2021. R: A Language and Environment for Statistical Computing. R Foundation for Statistical Computing, Vienna, Austria.
Ramsay, E.E., Fleming, G.M., Faber, P.A., Barker, S.F., Sweeney, R., Taruc, R.R., Chown, S.L., Duffy, G.A., 2021. Chronic heat stress in tropical urban informal settlements. iScience 24, 103248.
Ranagalage, M., Ratnayake, S.S., Dissanayake, D., Kumar, L., Wickremasinghe, H., Vidanagama, J., Cho, H., Udagedara, S., Jha, K.K., Simwanda, M., et al., 2020. Spatiotemporal variation of urban heat islands for implementing nature-based solutions: a case study of Kurunegala, Sri Lanka. ISPRS Int. J. Geo-Inf. 9, 461.
RISE & ADB, 2021. Water-sensitive informal settlement upgrading: Description of technologies. Asian Development Bank and Monash University.
Rose, N.L., Yang, H., Turner, S.D., Simpson, G.L., 2012. An assessment of the mechanisms for the transfer of lead and mercury from atmospherically contaminated organic soils to lake sediments with particular reference to Scotland, UK. Geochem. Cosmochim. Acta 82, 113–135.
Roy, D.P., Wulder, M.A., Loveland, T.R., Woodcock, C.E., Allen, R.G., Anderson, M.C., Helder, D., Irons, J.R., Johnson, D.M., Kennedy, R., et al., 2014. Landsat-8: science and product vision for terrestrial global change research. Rem. Sens. Environ. 145, 154–172.
Satterthwaite, D., Archer, D., Colenbrander, S., Dodman, D., Hardoy, J., Mitlin, D., Patel, S., 2020. Building resilience to climate change in informal settlements. One Earth 2, 143–156.
Scott, A.A., Misiani, H., Okoth, J., Jordan, A., Gohlke, J., Ouma, G., Arrighi, J., Zaitchik, B.F., Jjemba, E., Verjee, S., et al., 2017. Temperature and heat in informal settlements in Nairobi. PLoS One 12, e0187300.
Scovronick, N., Lloyd, S.J., Kovats, R.S., 2015. Climate and health in informal urban settlements. Environ. Urbanization 27, 657–678.
Sejati, A.W., Buchori, I., Rudiarto, I., 2019. The spatio-temporal trends of urban growth and surface urban heat islands over two decades in the Semarang Metropolitan Region. Sustain. Cities Soc. 46, 101432.
Seto, K.C., Shepherd, J.M., 2009. Global urban land-use trends and climate impacts. Curr. Opin. Environ. Sustain. 1, 89–95.
Simkin, R.D., Seto, K.C., McDonald, R.I., Jetz, W., 2022. Biodiversity impacts and conservation implications of urban land expansion projected to 2050. Proc. Natl. Acad. Sci. U.S.A. 119, e2117297119.
Simpson, G.L., 2018. Modelling palaeoecological time series using generalised additive models. Front. Ecol. Evol. 6, 149.
Simpson, G.L., 2022. gratia: Graceful 'ggplot'-based graphics and other functions for GAMs fitted using 'mgcv'. R Package Version 0.7.0-4. https://gavinsimpson.github.io/gratia/.
Sokal, R.R., Rohlf, F.J., 2012. Biometry : the Principles and Practice of Statistics in Biological Research, fourth ed. W.H. Freeman, New York.
Surya, B., Salim, A., Hernita, H., Suriani, S., Menne, F., Rasyidi, E.S., 2021. Land use change, urban agglomeration, and urban sprawl: a sustainable development perspective of Makassar City, Indonesia. Land 10, 556.
Tan, J., Zheng, Y., Tang, X., Guo, C., Li, L., Song, G., Zhen, X., Yuan, D., Kalkstein, A.J., Li, F., 2010. The urban heat island and its impact on heat waves and human health in Shanghai. Int. J. Biometeorol. 54, 75–84.
Tepanosyan, G., Muradyan, V., Hovsepyan, A., Pinigin, G., Medvedev, A., Asmaryan, S., 2021. Studying spatial-temporal changes and relationship of land cover and surface urban heat island derived through remote sensing in Yerevan, Armenia. Build. Environ. 187, 107390.
Tran, H., Uchihama, D., Ochi, S., Yasuoka, Y., 2006. Assessment with satellite data of the urban heat island effects in Asian mega cities. Int. J. Appl. Earth Obs. Geoinf. 8, 34–48.
Tran, K.V., Azhar, G.S., Nair, R., Knowlton, K., Jaiswal, A., Sheffield, P., Mavalankar, D., Hess, J., 2013. A cross-sectional, randomized cluster sample survey of household vulnerability to extreme heat among slum dwellers in Ahmedabad, India. Int. J. Environ. Res. Publ. Health 10, 2515–2543.
Trusilova, K., Jung, M., Churkina, G., 2009. On climate impacts of a potential expansion of urban land in Europe. J. Appl. Meteorol. Climatol. 48, 1971–1980.
Tuholske, C., Caylor, K., Funk, C., Verdin, A., Sweeney, S., Grace, K., Peterson, P., Evans, T., 2021. Global urban population exposure to extreme heat. Proc. Natl. Acad. Sci. U.S.A. 118, e2024792118.
U.S. Geological Survey, 2019. Landsat Collection 1 Level 1 Product Definition. Department of the Interior, Sioux Falls, South Dakota.
U.S. Geological Survey, 2020. Landsat 8 Collection 2 (C2) Level 2 Science Product (L2SP) Guide. Version 2.0. Department of the Interior Sioux Falls, South Dakota.
Un-Habitat, 2015. Issue paper on informal settlements. In: Habitat III Issue Papers. United Nations Conference on Housing and Sustainable Urban Development, New York.

United Nations, 2018. The worlds cities in 2018: data booklet. In: Population Studies. Department of Economic and Social Affairs, Population Division, United Nations, New York.
United Nations, 2019. World Urbanisation Prospects: the 2018 Edition. Department of Economic and Social Affairs, Population Division, United Nations, New York.
United Nations, 2021a. Indicator 11.1.1. In: Proportion of Urban Population Living in Slums (Percent). United Nations Human Settlements Programme). United Nations Department of Economic and Social Affairs SDG Indicators Database.
United Nations, 2021b. The Sustainable Development Goals Report 2021. Department of Economic and Social Affairs, United Nations Publications, New York, United States of America.
Van de Walle, J., Brousse, O., Arnalsteen, L., Brimicombe, C., Byarugaba, D., Demuzere, M., Jjemba, E., Lwasa, S., Misiani, H., Nsangi, G., et al., 2022. Lack of vegetation exacerbates exposure to dangerous heat in dense settlements in a tropical African city. Environ. Res. Lett. 17, 024004.
Venter, Z.S., Brousse, O., Esau, I., Meier, F., 2020. Hyperlocal mapping of urban air temperature using remote sensing and crowdsourced weather data. Rem. Sens. Environ. 242, 111791.
Venter, Z.S., Chakraborty, T., Lee, X., 2021. Crowdsourced air temperatures contrast satellite measures of the urban heat island and its mechanisms. Sci. Adv. 7, eabb9569.
Vicedo-Cabrera, A.M., Scovronick, N., Sera, F., Royé, D., Schneider, R., Tobias, A., Astrom, C., Guo, Y., Honda, Y., Hondula, D.M., et al., 2021. The burden of heat-related mortality attributable to recent human-induced climate change. Nat. Clim. Change 11, 492–500.
Wang, J., Kuffer, M., Sliuzas, R., Kohli, D., 2019. The exposure of slums to high temperature: morphology-based local scale thermal patterns. Sci. Total Environ. 650, 1805–1817.
Warton, D.I., Wright, I.J., Falster, D.S., Westoby, M., 2006. Bivariate line-fitting methods for allometry. Biol. Rev. 81, 259–291.
Whitmee, S., Haines, A., Beyrer, C., Boltz, F., Capon, A.G., de Souza Dias, B.F., Ezeh, A., Frumkin, H., Gong, P., Head, P., et al., 2015. Safeguarding human health in the Anthropocene epoch: report of the Rockefeller Foundation–Lancet Commission on planetary health. Lancet 386, 1973–2028.
Wickham, H., Francois, R., Henry, L., Muller, K., 2022. dplyr: a grammar of data manipulation. R package version 1.0.8. https://CRAN.R-project.org/package=dplyr.
Wong, T.H.F., Rogers, B.C., Brown, R.R., 2020. Transforming cities through water-sensitive principles and practices. One Earth 3, 436–447.
Wood, S.N., 2003. Thin plate regression splines. J. Roy. Stat. Soc. 65, 95–114.
Wood, S.N., 2004. Stable and efficient multiple smoothing parameter estimation for generalized additive models. J. Am. Stat. Assoc. 99, 673–686.
Wood, S.N., 2011. Fast stable restricted maximum likelihood and marginal likelihood estimation of semiparametric generalized linear models. J. Roy. Stat. Soc. B Stat. Methodol. 73, 3–36.
Wood, S.N., Scheipl, F., Faraway, J.J., 2012. Straightforward intermediate rank tensor product smoothing in mixed models. Stat. Comput. 23, 341–360.
Wulder, M.A., Loveland, T.R., Roy, D.P., Crawford, C.J., Masek, J.G., Woodcock, C.E., Allen, R.G., Anderson, M.C., Belward, A.S., Cohen, W.B., et al., 2019. Current status of Landsat program, science, and applications. Rem. Sens. Environ. 225, 127–147.
Yao, R., Wang, L., Huang, X., Gong, W., Xia, X., 2019. Greening in rural areas increases the surface urban heat island intensity. Geophys. Res. Lett. 46, 2204–2212.
Yu, Z., Xu, S., Zhang, Y., Jorgensen, G., Vejre, H., 2018. Strong contributions of local background climate to the cooling effect of urban green vegetation. Sci. Rep. 8, 6798.
Zaitchik, B.F., Tuholske, C., 2021. Earth observations of extreme heat events: leveraging current capabilities to enhance heat research and action. Environ. Res. Lett. 16, 111002.
Zhao, L., Oppenheimer, M., Zhu, Q., Baldwin, J.W., Ebi, K.L., Bou-Zeid, E., Guan, K., Liu, X., 2018. Interactions between urban heat islands and heat waves. Environ. Res. Lett. 13, 034003.
Zhou, B., Rybski, D., Kropp, J.P., 2017. The role of city size and urban form in the surface urban heat island. Sci. Rep. 7, 4791.
Zhou, D., Xiao, J., Bonafoni, S., Berger, C., Deilami, K., Zhou, Y., Frolking, S., Yao, R., Qiao, Z., Sobrino, J., 2018. Satellite remote sensing of surface urban heat islands: progress, challenges, and perspectives. Rem. Sens. 11, 48.
Zhu, Z., Zhou, Y., Seto, K.C., Stokes, E.C., Deng, C., Pickett, S.T.A., Taubenböck, H., 2019. Understanding an urbanizing planet: strategic directions for remote sensing. Rem. Sens. Environ. 228, 164–182.